ISSN 2063-5346 Section A-Research paper

UWB Transmitted Reference Receiver Based on Adaptive Dual-Tree Complex Wavelets Transform

Rashid Ali Fayadh[1]*
[1]*Associate Professor, Department of Electrical Engineering Techniques, Middle Teechnical University, Electrical Engineering Technical College, Baghdad, Iraq. Email: dr.rashidali@mtu.edu.iq
Nabil K. Al_Shamaa[2]
[2]Research Scholar, Department of Control Engineering Techniques, Electrical Engineering Technical College, Middle Technical University, Baghdad, Iraq. Email: nabilshamaa59@gmail.com
***Corresponding Author:** Dr. Rashid Ali Fayadh
*Associate Professor, Department of Electrical Engineering Techniques, Electrical Engineering Technical College, Middle Technical University, baghdad, Iraq. Email: rashidfayadh47@gmail.com

ABSTRACT

The Rake receiver has become very popular in wireless communication in recent years, but it has several drawbacks, including complexity, high noise, poor performance, and a slow transmission rate. As a result, a system with high performance, low complexity, low noise, and high efficiency is required. In this paper, a proposed adaptive transmitted reference receiver with dual-tree complex wavelet transform (DTCWT) was produced and analyzed by complex discrete wavelet transform (DWT). This proposed receiver achieves high performance, low complexity, higher transmission rate, and lower noise than previous rake receivers or wavelet transform systems. High frequencies that caused noise in the system were cut off using DWT. To remove these frequencies, DTC-DWT uses two types of FIR filters. To get a better result, use three levels in this system. A maximal ratio combiner (MRC) is used to capture most of the multipath components, and an adaptive filter of recursive least squares (RLS) is used to update MRC input. High gain UWB antenna was applied as single-in multi-out (SIMO) and multi-in multi-out (MIMO) to give a more powerful link for data to maximize channel capacity. The simulation results show that when dual-tree complex filters of three levels of noise reduction are used, the effect is to remove high frequencies that cause noise in the TR UWB received signal. The bit error probability is reduced according to the peak-average-power ratio (PAPR) compared with the conventional transmitted reference (TR) receiver.

Keywords : PAPR, DTC-WT_UWB receiver, channel capacity, RLS adaptive filter, multipath components

1.0 Introduction

The bandwidth of the UWB (Ultra Wide Band) communications system is from 3.1 to 10.6) GHz. The bandwidth of UWB will be given a chance for very high data rate communications. There are two types of applications for UWB based on data rates: low data rate applications and high data rate applications. In UWB techniques, the different impulses are assumed for low power, low complexity, and low data rate application. There is some challenge for UWB transceiver, low power and low cost [1]. The Rake receiver of UWB is highly complex because it consists of several fingers, so the system performance is lost [2].
It subsequently proposed a new system known as transmitter reference Ultra-wideband (TR-UWB) receiver that has some advantages such as low complexity until it has known a low-complexity alternative to rake receiver, less noise, higher transmission rate, no channel estimation and no need to generate a pulse in the receiver with information data as compared with the rake receiver [3, 4]. Nevertheless, this type has some disadvantages, such as it cannot efficiently reduce the noise of received signal, so a new type of receiver is proposed to remove noise.
Many papers have been published on using Wavelet Transform (WT) to overcome low complexity for receivers. WT in UWB communication has been used to synthesize and analyze the UWB signal to create the signal needed for noise detection [5, 6]. WT was also used to diagnose breast cancer using UWB contact [7]. The Wavelet Transform is a modern mathematical technique for compressing signals and

images and eliminating noise from their coefficients [8, 9]. The wavelet video pressure was evaluated for multi-carrier, multiple access, wideband, code division, and a rake receiver over additive [10, 11]. In [12], Continuous Wavelet Transform (CWT) was used in the rake receiver, which showed a significant improvement in performance and a less complex receiver.

This paper used Dual-Tree Complex Wavelet Transform (DTCWT) based on an adaptive TR receiver that contains Low Pass Filter (LPF) and High Pass Filter (HPF). A part of LPF is used only to cut off high frequencies that cause internal noise for the TR-UWB receiver and then procure the received signal with less deformity. This receiver depends on the wavelet signal decomposition algorithm, which divides the signal into three levels and generates approximated and detailed coefficients. A maximal ratio combiner (MRC) was used to combine the train of received signals from multipath (line of side and non-line of side) to support the amplitude of a required signal. To minimize the MSE (mean squared error), an algorithm of recursive least squares (RLS) is applied in the adaptive filter to update the weak input coefficients of the combiner.

The rest of this paper is structured as follows: section two presents a system model analysis. While section three detailed the wavelet transform process. The transmitted Reference (TR) system is the subject of section four. Sections five and six deal with proposed TR receiver performance and channel capacity. In addition, sections seven and eight analyze simulation results with their discussions and conclusions, respectively.

2.0 System Model for Transmission and Reception Bits

The model is shown in Fig. 1 with UWB-generated binary symbols (S= ± 1) transmitted as a train of ultra-short pulses. The pulse shape is a Gaussian pulse of 2nd derivatives modulated by binary phase shift keying (BPSK). Transmission is repeated over the number of frames (N_f). Each takes a time duration of T_f, and the symbol time (T_s) is $T_s = N_f \times T_f$ [13]. The UWB indoor channel contains multipath propagation over the line of side (LOS) and non-line of side (NLOS). The UWB transmitted reference system must capture most of the multipath components of satisfactory resolution, which arrived in clusters and rays caused by indoor obstacles, as shown in Fig. 2 [14]. According to the strength of each path, there is a technique to combine the match filter output signals called maximal ratio combining (MRC). This technique combines the current symbols after correcting the phase rotation caused by channel fading before the decision circuit. The PAPR is the ratio of signal power (P_s) and noise power (P_n) over Ts duration and can be calculated by the following equations [15].

$$\mathrm{PAPR_{MRC}} = \frac{P_s}{P_n} = \sum_{n=1}^{N} \frac{E_b}{N_o} h_n \qquad (1)$$

where E_b is transmitted bit energy, No is the noise power spectral density of AWGN, and hn is the gain of N-th paths. The channel power ratio over N elements of the path is measured below:

$$\mathrm{CPAPR_{MRC}} = \sum_{n=1}^{N} (\mathrm{PAPR_{MRC}})_n \qquad (2)$$

In the system, an adaptive filter is connected to the output of the combiner to maximize the PAPR with an impulse response of h(T-t). The matched filter is sampled at t=T and $0 \leq t \leq T$, containing the desired signal and noise component.

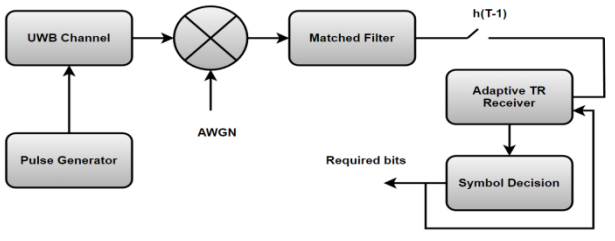

Figure. 1 TR System Model

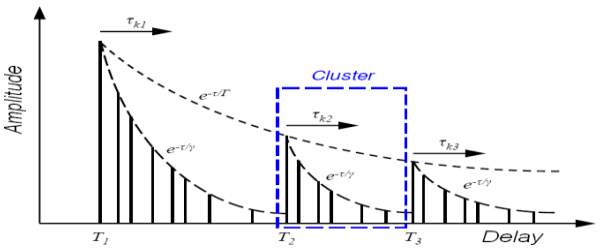

Figure. 2 Wireless AWGN channel model.

3.0 **Wavelet Transform Process**

The wavelet transform was introduced by Morletetal and displayed at the start of 1980. Morletetal used the wavelet transform to estimate seismic data. The wavelet theory is distinguished from the Fourier theory. It can express a signal of Fourier theory, such as the added compilation of cosines, sines, and possibly infinite. This sum can express Fourier expansion. The Fourier expansion has a significant disadvantage, it has no time resolution, but it has frequency resolution. At the same time, the problem of Fourier theory cannot define both frequency and time domains for signal [16]. Later, different kinds of wavelet transform were developed and found plentiful implementations, such as continuous time wavelet transform (CWT). The discrete wavelet transform (DWT) has distinguished signal compaction characteristics for many real-world signals while the calculation is extraordinarily active. Therefore, it has been utilized in nearly every technical domain, including pattern recognition, denoising, numerical integration, and image compression. The wavelet transform has a goal: defining signals such as linear conjunction of functions for the wavelet at sundry scales and functions for scaling the broadest asked scale. The goal of the wavelet is to transpose the signal from the time domain to the time-scale domain (time-frequency) that decides the subscriber time with frequency [17]. It involves specific kinds of waves to define the signal. These are called wavelets. For CWT analysis, the signal can be defined as decay into wavelets that can be expressed below:

$$\mathrm{CWT} = \mathrm{b}(\mathrm{s},\tau) = \int \mathrm{f}(\mathrm{t}).\psi_{\mathrm{s},\tau} * (\mathrm{t})\mathrm{dt} \qquad (3)$$

$$\mathrm{ICWT} = \mathrm{f}(\mathrm{t}) = \int\int \mathrm{b}(\mathrm{s},\tau).\psi_{\mathrm{s},\tau}(\mathrm{t})\mathrm{ds}\,\mathrm{d}\tau \qquad (4)$$

where * is the denoted difficult conjunction, f(t) is decayed into group of rule functions, $\psi_{s,\tau}(t)$=named the wavelet signal. s, τ are incoming dimensions. The wavelet transform has t many essential attributes, such as the systematic, stipulations, and permissibility that express below.

$$\int_{-\infty}^{\infty} \frac{|\psi(w)|^2}{|w|}\ \mathrm{dw} < +\infty \qquad (5)$$

The DWT reduces the calculation time and supplies information during synthesis and analysis operations. The WT consists of two kinds of filters used to the cutoff frequency that cause signal noise. There are two types of filters, HPF used to cutoff low frequencies and LPF used to cutoff high frequencies, as shown in Figure (1). Used filters to confirm the signal degeneration by varying the scale by a factor (j) as expressed below [18].

$$\mathrm{h}[\mathrm{j}] = \sum_{\mathrm{i}=-\infty}^{\infty} \mathrm{x}[\mathrm{j}].\mathrm{h}[\mathrm{j}-\mathrm{i}] \qquad (6)$$

$$\mathrm{r}[\mathrm{j}].\mathrm{g}[\mathrm{i}] = \sum_{\mathrm{i}=\infty}^{\infty} \mathrm{x}[\mathrm{j}].\mathrm{g}[\mathrm{j}-\mathrm{i}] \qquad (7)$$

where, h[i] is the impulse response of LPF and g[i] is the impulse response of HPF.

$$\mathrm{Y}_{\mathrm{high}}[\mathrm{i}] = \sum_{\mathrm{j}} \mathrm{x}[\mathrm{j}].\mathrm{g}[2\mathrm{i}-\mathrm{j}] \qquad (8)$$

$$\mathrm{Y}_{\mathrm{Low}}[\mathrm{i}] = \sum_{\mathrm{j}} \mathrm{x}[\mathrm{j}].\mathrm{h}[2\mathrm{i}-\mathrm{j}] \qquad (9)$$

While the inverse of the wavelet transform (IDWT) makes building on the relation between the HPF and LPF, which can be defined below.

$$\mathrm{x}[\mathrm{j}] = \sum_{\mathrm{i}=-\infty}^{\infty(} \left(\mathrm{Y}_{\mathrm{high}}(\mathrm{i}).\mathrm{g}[-\mathrm{j}+2\mathrm{i}]\right) + (\mathrm{Y}_{\mathrm{low}}(\mathrm{i}).\mathrm{h}[-\mathrm{j}+2\mathrm{i}]) \qquad (10)$$

$$\mathrm{g}[\mathrm{D}-1-\mathrm{j}] = (-1)^{\mathrm{j}}.\mathrm{h}[\mathrm{j}] \qquad (11)$$

where (-1) is translated from LPF to HPF, D is the filters' tallness.

The dual-tree complex wavelet transform (DTCWT) enhances DWT with additional properties, shifting invariant and direct selection to two or more dimensions. So the transformation comprises two parallel DWT filter banks. The design of a complex dual-tree is shown in Fig. 3, which gives 2N points of DWT coefficients to make tree A and tree B over three levels of high pass and low pass filters of order 10. Tree A signals act as real parts of complex transform, and tree B signals act as imaginary components [19].

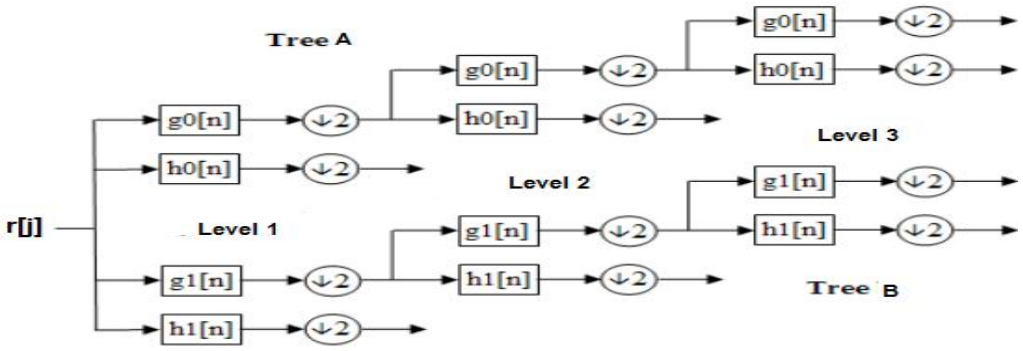

Fig. 3 HPF and LPF of dual-tree architecture.

4.0 **Transmitted Reference (TR-UWB) System**

In this wireless system, the used pulse is based on a second derivative Gaussian pulse p(t) can express in equation (10). The Gaussian pulse has a zero DC component. The Gaussian pulse is chosen over a rectangular pulse because it has less energy outside the allocated frequency band [20].

$$p(t) = \left[1 - 4\pi\left(\left(t - \frac{0.35}{\tau_m}\right)^2\right)\right]\exp\left[-2\pi\left(\left(t - \frac{0.35}{\tau_m}\right)^2\right)\right] \qquad (12)$$

The TR signaling technique consists of an unmodulated reference signal and a modulated data signal for each information bit. In conventional TR systems, the modulated signal is transmitted after an unavoidable delay following the unmodulated signal to ensure no interference between the two signals. A Binary Phase Shift Keying (BPSK) modulated TR signal pair is below.

$$s_0(t) = g_{tr}(t) + b_0 g_{tr}(t - T_d) \qquad (13)$$

where $g_{tr}(t)$ is represents an ultra-wideband pulse with a non-zero value in the interval $[0, T_m]$; the energy of $g_{tr}(t)$ is defined as $\frac{E_b}{2}$ and $b0$ € {-1,1}. A binary PSK-modulated TR signal pair is illustrated in Fig. 4. In this research, the delay T_d between the unmodulated and modulated pulses is set to equal the data transmission time frame T_f . Therefore, TR signal pairs are transmitted at intervals of $2T_f$. To improve transmission reliability, the same TR signal pair can be sent. N_s Times. The circuit of the TR-UWB transmitter signal can be shown in Fig. 5 and represented below [21].

$$s_{tr}(t) = \sum_{i=\infty}^{\infty} g_{tr}\left(t - 2iT_f\right) + b_{\lfloor \frac{i}{N_s} \rfloor} g_{tr}(t - (2i+1)T_f) \qquad (14)$$

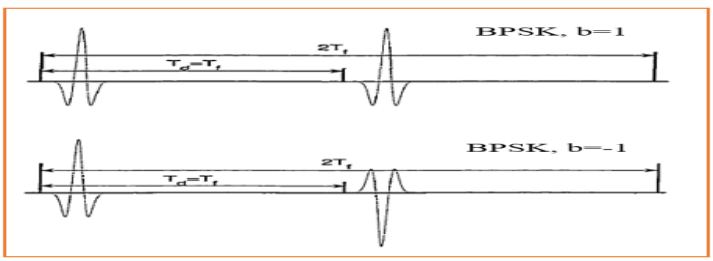

Figure. 4 The BPSK modulated TR system signal pair.

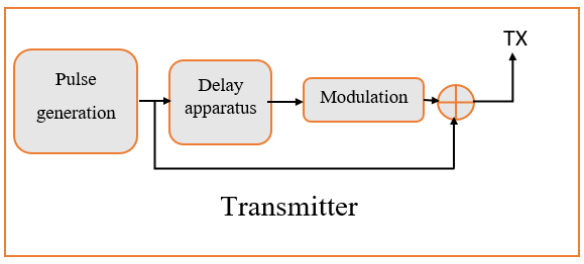

Figure. 5 TR-UWB transmitter.

ISSN 2063-5346 *Section A-Research paper*

Since the unmodulated signal is transmitted together with the modulated signal as a pair on the same channel, the unmodulated signal will undergo the same channel distortion as the modulated signal assuming the channel remains unchanged during the period. T_f [22]. Thus, the received unmodulated signal can be used as a noisy reference to detect the modulated signal and avoid the need for explicit channel estimation. The received signal pair is expressed in the equation below. The channel receiver signal will go to the transmitted reference receiver [23].

$$\bar{r}_{tr}(t) = \sum_{i=\infty}^{\infty} g_{tr}\left(t - 2iT_f\right) + b_{\lfloor \frac{i}{N_s} \rfloor} g_{tr}\left(t - (2i+1)T_f\right) + \bar{n}(t) \qquad (15)$$

where $\bar{n}(t)$ is the zero mean additive white Gaussian noise (AWGN) with variance $\frac{N_0}{2}$

5.0 The Proposed Transmitted Reference (TR.) Receiver Performance

Two TR receiver designs are analyzed in this section: conventional TR receiver and adaptive DTCWT transmitted reference receiver based on 3 levels of DWT.

5.1 Conventional transmitted reference (TR-UWB) receiver

The received signal is passed through an ideal low pass filter with a one-sided bandwidth of W and unit magnitude at the receiver. The output of the low pass filter at the *i*th symbol interval (with duration *2NsTf)* can be expressed in the equation below.

$$r_i(t) = \sum_{j=0}^{N_s-1} [g_{rx}\left(t - 2jT_f\right) + b_i g_{rx}(t - (2i+1)T_f)] + \bar{n}(t) \qquad (16)$$

where $g_{rx}(t)$ corresponds to the received pulse shape. The use of different representations for pulses is to indicate the possible shape difference between the received $g_{rx}(t)$ and the transmitted pulse $g_{tr}(t)$ due to channel distortion. The bandwidth of the low pass filter is designed to limit the white Gaussian noise to within the filter bandwidth and allow the pulse pair to pass through without distortion. The term $n(t)$ indicates the band-limited noise. The following section will present two autocorrelation detectors and their performance analysis. Autocorrelation correlates the unmodulated reference signal with the modulated data signal to demodulate the data signal. The autocorrelation takes the received signal $r_{tr}(t)$ and multiply it with a T_f Delayed received signal and integrated it over some time $T_{tr}(t)$ [24]. The proposed circuit of the TR-UWB receiver can be shown in Fig. 5. The autocorrelation output for one symbol duration is expressed below [25].

$$D = \sum_{j=0}^{N_S-1} \int_{(2j+1)T_f+T_{tr}}^{(2j+1)T_f+T_{tr}} r_i(t) r_i(t - T_f) dt$$

$$= \sum_{j=0}^{N_s-1} \int_{(2j+1)T_f+T_{tr}}^{(2j+1)T_f+T_{tr}} \left\{ \left[\left[g_{rx}\left(t - 2jT_f\right) + b_i g_{rx}\left(t - (2j+1)T_f\right] + n(t) \right) \right] . \left[\left[g_{rx}\left(t - 2jT_f\right) + b_i g_{rx}\left(t - (2j+1)T_f - T_f\right) \right] + n\left(t - T_f\right) \right] dt \qquad (17)$$

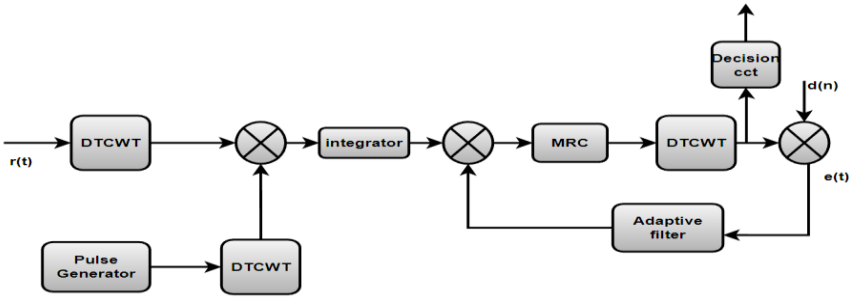

Fig. 5 The Proposed DTCWT-based adaptive transmitted reference receiver architecture.

The variance exists when a=j and $v = t - (2j-1)T_f$ Can express bellow.

$$\sigma_{X_4}^2 \approx \sum_{J=0}^{N_s-1} \int_0^{T_{tr}} \int_0^{T_{tr}} R_n^2(v_2 - v_1) dv_1\, dv_2 \quad (18)$$

$$\sigma_{x_4}^2 \approx N_s W \frac{N_0^2}{2} T_{tr} \quad (19)$$

To decision, variable D can then be an approximate Gaussian RV conditioned on the bit and τ . Its mean and variance are expressed below [25].

$$E[D|b_i, \tau] = N_s b_i R(0) \quad (20)$$

$$Var[D|\tau] = N_S N_0 R(0) + \sigma_{X_4}^2 \quad (21)$$

where,

$$R(\tau) = \int_0^{T_{tr}} g_{rx}(t) g_{rx}(b - \tau) dt \quad (22)$$

The conditional probability of error for the autocorrelation receiver can express below.

$$P(e|\tau) = P(D < 0|b_i = 1, \tau) = Q\left(\frac{N_S R(0)}{\sqrt{N_S N_0 R(0) + \sigma_{X_4}^2}}\right) \quad (23)$$

At the output of the combiner, an adaptive filter is connected to maximize the power ratio using the RLS algorithm to reduce the difference (e(n)) between desired signal (d(n)) and the model filter output. So, in every iteration, there is an update to the adaptive filter weights by the recursive form of the cost function ($J_{(n)}$).

$$J(n) = \sum_{i=0}^{n} \lambda^{n-i}\ (e(n))^2 \quad (24)$$

Where e(n) is the error signal, and λ ($0 \leq \lambda \leq 1$) is the forgetting factor. To calculate the output signal of the adaptive filter with combiner out (Y(n)) and desired signal (d(n), follow the bellow equations:

$$e(n) = d(n) - Y(n) \quad (25)$$

At the adaptive filter coefficients vector of $W(n) = [w_1(n), w_2(n),--------w_M(n)]^T$ and input signal information vector of

$$r(n) = [r(n), r(n-1), r(n-2),-----r(n-m)]^T \quad (26)$$

$$Y(n) = r^T(n)\, W(n) \quad (27)$$

To recursively update the values of w(n) according to the RLS algorithm and Kalman gain vector (K(n)), the filter coefficients are changing and controlling each tap coefficient.

$$W(n) = w(n-1) + K(n)\, \alpha(n) \quad (28)$$

where $\alpha(n) = d(n) - r^T(n)\, w(n-1)$ (29)

5.2 Dual-Tree complex transmitted reference (DTCTR-UWB) receiver

In this system, the proposed DTCTR – UWB receiver is based on DWT because all applications need a system with low cost and reduced complexity. This circuit is based on DWT and can be shown in Fig. 6. For starters, remove some components that can build a system without having to, such as LPF, Amplifier, Integrator, and Decision output. Thus, propose a system with no significant component; this component is not expensive. Autocorrelation correlates the unmodulated reference signal with the modulated data signal

to demodulate the data signal. The autocorrelation takes the received signal. $r_{tr}(t)$ and multiply it with a T_f Delayed received signal and the autocorrelation can be expressed as below.

$$D = \sum_{j=0}^{N_S-1} r_i(t) r_i(t - T_f) dt$$

$$= \sum_{j=0}^{N_s-1} \{ [g_{rx}(t - 2jT_f) + b_i g_{rx}(t - (2j+1)T_f)] + n(t)]$$

$$. [g_{rx}(t - 2jT_f - T_f) + b_i g_{rx}(t - (2j+1)T_f - T_f) + n(t - T_f)]\} \quad (30)$$

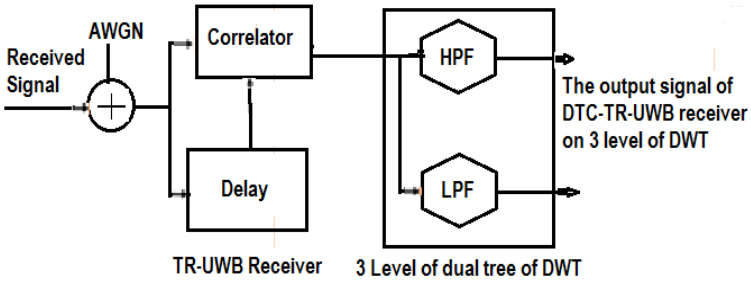

Fig. 6 The Circuit of DTC-TR-UWB Based on DWT.

After that, Integrator and Decision output were removed, and 3 levels of DWT were used. The DWT consists of two types of filters HPF and LPF. In this receiver, we need to analyze high frequencies. So, these levels can express below by using only LPF for 3 levels of DWT to remove high frequencies that caused the noise signal.

$$cA1 = \sum_{K=0}^{L} h(k) D(2n + k), level\ 1\ of\ DWT \quad (31)$$

$$cA2 = \sum_{K=0}^{L} h(k)\ cA1(2n + k)\ , level\ 2\ of\ DWT \quad (32)$$

$$cA3 = \sum_{K=0}^{L} h(k)\ cA2(2n + k), level\ 3\ of\ DWT \quad (33)$$

6.0 Channel Capacity at Single and Multiple Antennas

For the application of this proposed receiver, the system was simulated over Rayleigh channel fading through indoor propagation. As the bit rate of communication plays a crucial role, the performance of channel capacity has to be shown. The antenna's gain is one of the most important benefits of a wireless system: it increases the channel's capacity without adding extra bandwidth or increasing the signal power at the transmitter. Increasing the channel's capacity will support improving the multiple-input multiple-output (MIMO) technique in transmitters and receivers, reducing the bit error probability. In a MIMO system, two random signal vectors were considered, one for the input signal (s) to the channel and one for the output signal (q) from the channel. Depending on Fig. 7 shows the configurations of the selected antennas at both sides of transmission and reception. As the UWB power is -41.3 dBm\MHz or 75 nW\MHz, the antenna of high gain reflectors (11-18) dB is used to cover the dual polarization of SIMO and MIMO systems [26, 27].

$$Q = H\ s + w \quad (34)$$

where $s = [s_1, s_2, s_3, \ldots . s_M]^T$ is the transmitted signal vector up to M (number of omnidirectional transmitted antennas), $q = [q_1, q_2, q_3, \ldots . q_N]^T$ is the received signal vector up to N (the number of

omnidirectional received antennas), w is the Gaussian noise vector with zero mean and equal variance, and H is the M x N channel matrix.

$$H = \begin{bmatrix} h_{1,1} & \cdots & h_{1,N} \\ \vdots & \ddots & \vdots \\ h_{M,1} & \cdots & h_{M,N} \end{bmatrix} \qquad (35)$$

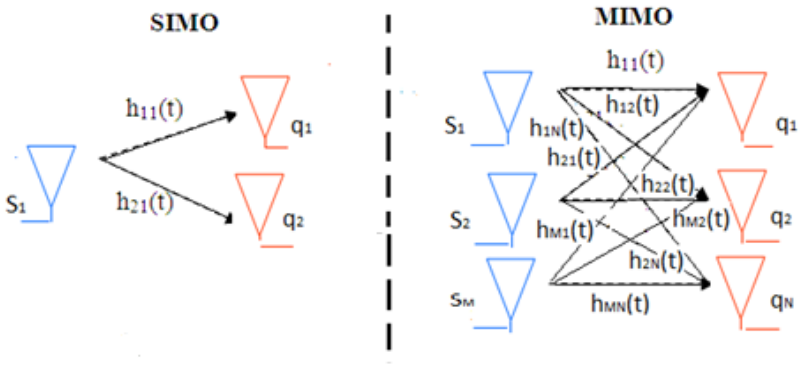

Fig. 7 Configuration of single and multiple antennas.

Assuming that the channels are noiseless means that their realizations are independent. The capacities of the SIMO and MIMO systems (bits per sample) for indoor and UWB wireless bandwidth (B) are given by [28]:

$$C_{SIMO} = B\,Log_2\,(1 + PAPR\,\sum_{n=1}^{N}\lambda_n) \qquad (36)$$

$$C_{MIMO} = L \times B\,Log_2\,(1 + \lambda \times PAPR) \qquad (37)$$

where L is the number of channels, PAPR is the peak-to-average-power ratio, and λ is a non-zero eigenvalue of the M x N matrix. The PAPR at the receiving antennas is defined as the ratio of the desired power of the received signal to the noise plus interference power so that the PAPR is related to and is proportional to antenna gain G(θ, ϕ) when the noise distribution is uniform, where θ is the elevation angle, and ϕ is the azimuth angle for the antenna radiation patterns [29].

7.0 Simulation Results and Discussions

7.1 Data pulses in the receiver

The proposed system produces reference pulses and two types of pulse data, with only the reference pulse being modulated. Fig.7 (a) shows the magnitude of the pulses in the time spectrum, and (b) illustrates the noise signal through the AWGN channel. Fig. 7(c) shows that the channel spectrum contains data pulse for noise and information signals, and (d) represents the spectrum of the correlator signal phase. Fig. 8(a) shows the time spectrum of the received signal, and after subtracting or separating the reference pulse from the data signal, Fig. 8(b) illustrates the precise pulses for the proposed system, which leads to a reduced probability of bits error and to decrease incorrect bits.

ISSN 2063-5346 *Section A-Research paper*

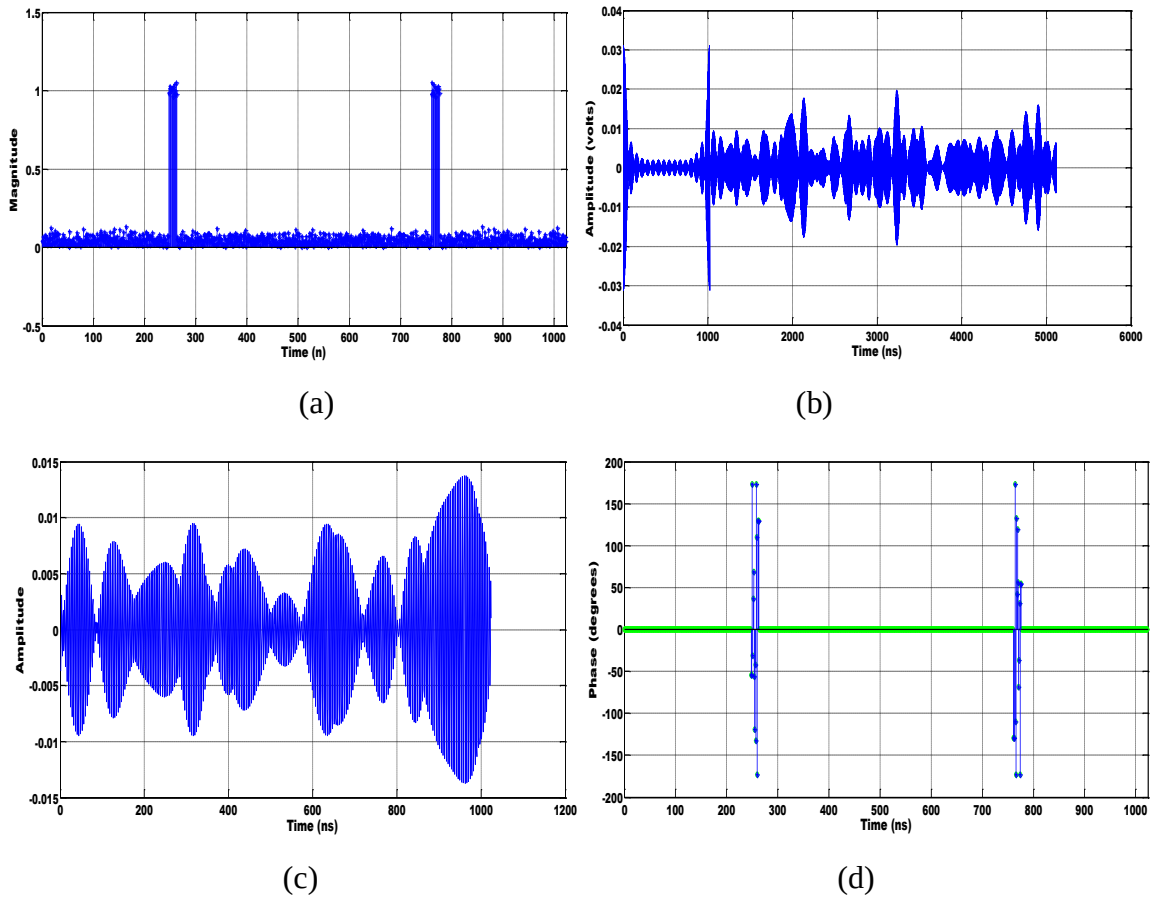

(a) (b)

(c) (d)

Fig. 7. (a) The magnitude of the received noisy spectrum, (b) Amplitude of noisy time signal, (c) Time signal, one symbol period, and (d) The carrier signal phase.

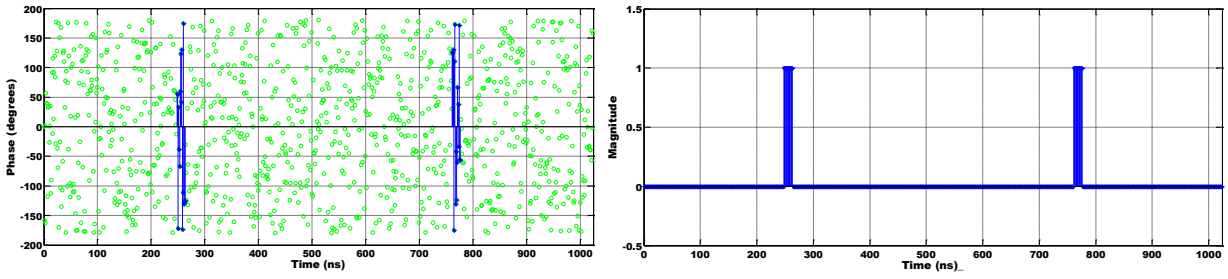

(a) (b)

Figure. 8 (a) The spectrum of the received signal, and (b) The magnitude of the carrier signal.

7.2 Cumulative distribution function (CDF) probability results

Three DTC-DWT levels were used to reduce the noise in the output of the received signal. Fig. 9(a) shows the CDF of the original signal versus PAPR, which is 15 dB at zero CDF. Fig. 9(b) shows the evaluated signal with reduced noise with no adaptive filter, and (c) shows the PAPR reduction level of 5.5 dB at zero CDF with an adaptive filter. The proposed adaptive system has superiority in reducing PAPR, which is 9.5 dB, to be more suitable in the design of the UWB TR receiver.

ISSN 2063-5346

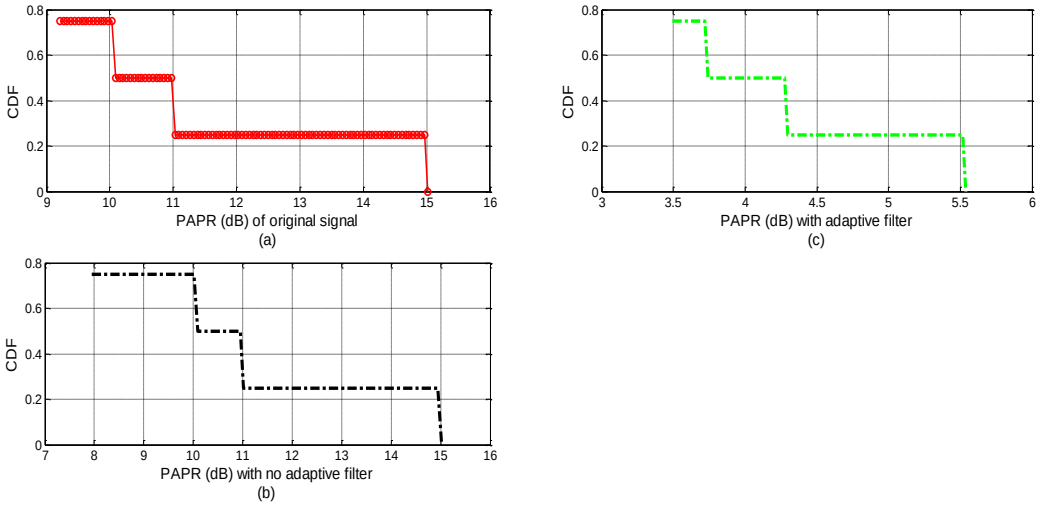

Fig. 9 (a) The original signal of TR-UWB, (b) The signal with no adaptive filter, and (c) the signal with an adaptive filter.

7.3 Channel capacity simulation results

Over Rayleigh fading channel, Fig. 10 and Fig. 11 show the proposed system characteristics with high gain microstrip wireless UWB antenna are connected in an array to illustrate SIMO and MIMO scenarios. The CDF is increasing to maximize the channel capacity indicated in bits per sample with PAPR equal to 5 dB, and increasing bit rates of indoor wireless communication evidence multiple antennae at the transmitter and receiver.

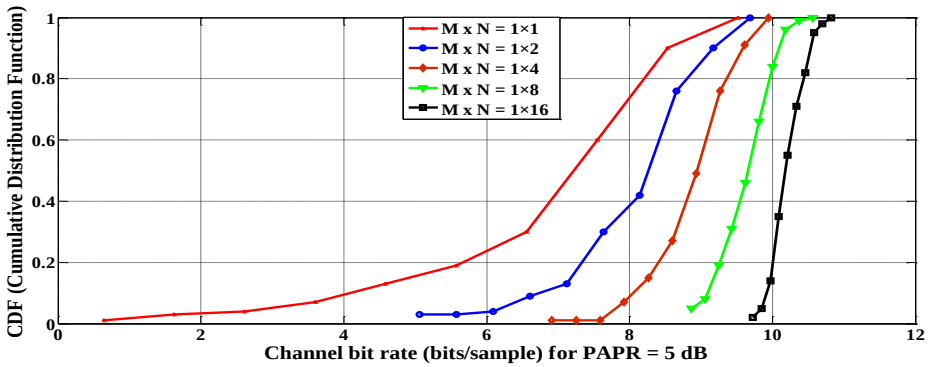

Fig. 10 CDF versus channel bit rate for SIMO channels with M x N and PAPR = 5 dB.

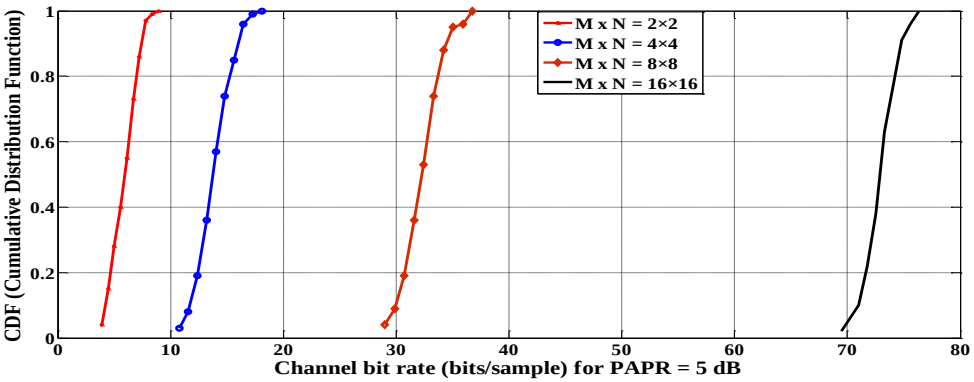

Fig. 11 CDF versus channel bit rate for MIMO channels with M x N and PAPR = 5 dB.

ISSN 2063-5346 *Section A-Research paper*

7.4 Probability of bit error reduction results

The performance analysis of the proposed system is shown in Fig. 12 and Fig. 13 in terms of the probability of bits error versus PAPR ratio in dB for conventional TR, TR with complex wavelet transform (CWT), and adaptive DTCWT receivers. The simulation was done with generated random Gaussian pulses (2^{nd} derivative) of 0.5 ns width and frame duration of 20 ns with 0.05 ns sampling interval and 10 pulses per frame. The gain of using CWT is 3.5 dB at an error probability of $10^{-3,}$ while that of using DTCWT is 6 dB at an error probability of 10^{-3} compared with conventional TR receivers. So, the performance of the TR-CWT receiver is improved by almost 2.5 dB PAPR when applying dual-tree complex filters.

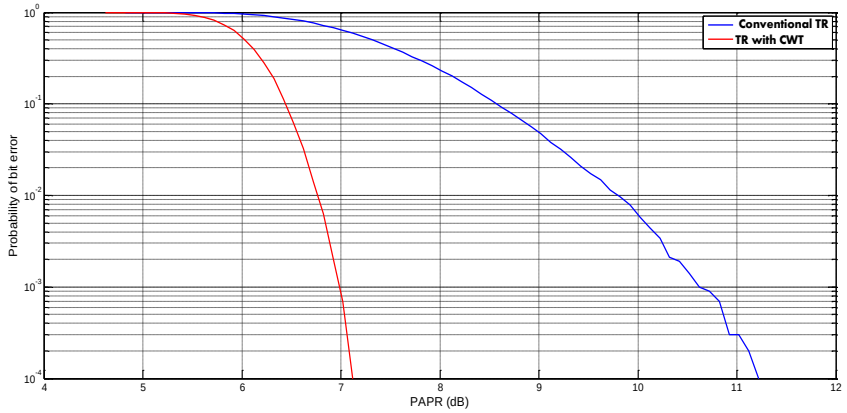

Figure. 12 The probability of bit error performance for conventional TR and TR-CWT.

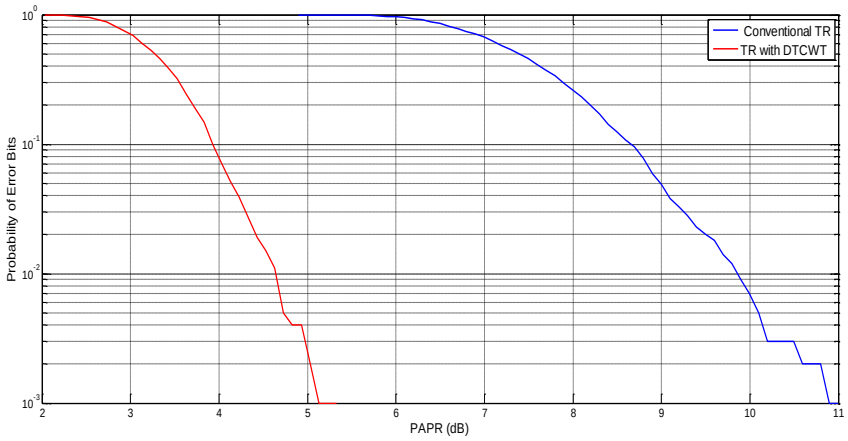

Fig. 13 The probability of bit error performance for conventional TR and adaptive TR-DTCWT.

8.0 Conclusions

As can be seen from the output received signal, it contains noise, bit error, and is very fuzzy. As a result, a new system based on the DWT known adaptive DTCWT- TR UWB system was proposed. This system employs dual-tree complex DWT, comprising LPF and HPF filters. The LPF was then used in all levels of DWT to obtain the output of the received signal with very little, high relief, and minimal disruption. Also, because there is no need for channel estimation, amplifier, and pulse generation at the receiver, this system does not require extensive or expensive components.

Furthermore, the adaptive TR receiver is low in cost, low in power, and light in weight. MRC was used to combine the maximal ratio of the out signals of the integrator and the adaptive filter of the RLS algorithm to support the weak input signal of MRC. This proposed research improved capturing of the signal energy at different components. So, the performance of this proposed receiver is evaluated by a PAPR gain of an average of 3.5 – 6 dB compared with a conventional transmitted reference receiver. As an application of

this proposed receiver with a high gain antenna, the channel capacity was increased at SIMO and MIMO cases to make this system more suitable for indoor propagation of UWB applications.

References

1. ILIE Florentin, "Discussion on UWB Technology and Its Applicability in Different Fields," Journal of Military Technology, Vol. 4, No. 1, pp. 29-34, 2020.

2. R. A. Fayadh, M. K. Wali, D. Y. Altaee, "Transmitted reference UWB wireless receiver based on FFT technique", International Journal of Advanced Technology and Engineering Exploration, Vol. 4, No. 34, pp. 136-11, 2017.

3. M. E. Tutay and S Gezici, "Optimal and Suboptimal Receivers for Code Multiplexed Transmitted-Reference Ultra-Wideband Systems", *Wireless Communications and Mobile Computing*, Vol. 13, pp. 1435-1449, 2013.

4. `Y. Jin, H. Liu, K. J. Kim and K.S. Kwak, "A Reconfigurable Digital Receiver for Transmitted Reference Pulse Cluster UWB Communications", *IEEE Trans. on Vehicular Technology*, Vol. 63, pp. 4734~4740, 2014.

5. Emmanuel, N. X. Fernando "Wavelet-Based Spectral Shaping of UWB Radio Signalfor Multisystem Coexistence", *Computers and Electrical Engineering Journal*, Vol. 36, No. 2, 2010.

6. B. Liu and W. Chang, "A Novel Range- Spread Target Detection Approach for Frequency Stepped Chirp Radar", *Progress in Electromegnatic Research*, Vol. 131, pp. 275-292, 2012.

7. B. McGinley, M. O'Halloran, R. Conceicao, G. Higgins, E. Jones, and M. Glavin1, "The Effect of Compression on Ultra Wideband Radar Signal", *Progress in Electromegnatic Research*, Vol. 117, pp. 51-65, 2011.

8. F. Khan, A. Ghafaar, N. Khan, and S. Ho Cho, "An Overview of Signal Processing Techniques for Remote Health Monitoring Using Impulse Radio UWB Transceiver", *Sensors*, Vol. 20, No. 9, pp. 2479, 2020.

9. M. Iqbal, Jie Chen, Wei Yang, Pengbo Wang, and Bing Sun, "SAR Image Despeckling by Selective 3D Filtering of Multiple Compressive Reconstruction Images", *Progress in Electromegnatic Research*, Vol. 134, pp. 209-226, 2013.

10. M. Hung Le and N. E. Mastorakis, "Performance Analysis of Wideband MCCDMA for Wavelet Vidio with Multilevel UEP Code over Fading Channels", *5th WSEAS INT Conf. Corfu, Greece*, pp 114-119, 2015.

11. Y. N. You, H. P. Xu, C. S. Li, and L. Q. Zhang, "Data Acquisition and Processing of Parallel Frequency SAR Based on Compressive Sensing", *Progress in Electromegnatic Research*, Vol. 133, pp.199-215, 2013.

12. I. Amera Zaki, S. E. El-Khamy and E. F. Badran, "A Novel Rake Receiver Based on continuous Wavelet Transform Designed for UWB Systems", *European Journal of Scientific Research*, Vol. 83, No.4, pp 463-474, 2012.

13. R. A. Fayadh, F. Malek, Hilal A. Fadhil, Sameer K. Salih, and Farrah Salwani Abdullah, "Design of A UWB Wireless Indoor Rake Receiver Using Continuous and Discrete Wavelet Transform Approaches", *Journal of Theoretical and Applied Information Technology*, Vol. 61, No.1, 2014

14. Ch. Navitha, K. Sivani, K. Ashoka Reddy, "Performance Evaluation of Adaptive Continuous Wavelet Transform based Rake Receiver for UWB Systems", *International Journal of Electrical and Computer Engineering (IJECE)*, Vol. 8, No. 5, pp. 3444~3452, 2018.

15. R. A. Fayadh, F. Malek, Hilal A. Fadhil, N. A. Mohd Affendi, Azuwa Ali, and M. F. Haji Abd Malek, "Adaptive Rake Receiver Using Matched Filter with Three Combining Techniques", *Australian Journal of Basic and Applied Sciences*, Vol. 7, No. 5, pp. 26-33, 2013.

16. Q. Dang, A. Trindade, A.-J. Van Der Veen, and G. Leus, "Signal Model and Receiver Algorithms for A Transmit Reference Ultra-Wideband Communication System", *IEEE Journal on Communications*, Vol. 24, No. 4, pp.773–779, 2006.

17. Dr. Mousa K. Wali, Dr. Rashid A. Fayadh, D. Y. Al_taee, "Performance of AWGN and fading channels on wireless communication systems using several techniques", *International Journal of Wireless Communications and Networking Technologies*, Vol.6, No.3, pp.19-23, 2017.

18. M. Farhang and J. A. Salehi, "Optimum Receiver Design for Transmitted-Reference Signaling", *IEEE Transaction Communication*, Vol. 5, pp. 1589-1598, 2010.

19. M. E. Tutay and S Gezici, "Optimal and Suboptimal Receivers for Code-Multiplexed Transmitted-Reference Ultra-Wideband Systems", *Wireless Communications and Mobile Computing*, Vol. 13, pp. 1435-1449, 2013.

20. Y. Jin and K. S. Kwak, "A Transmitted Reference Pulse Cluster Averaging UWB Receiver", *IEEE Systems Journal*, pp. 1932-8184, 2014.

21. H. Monga, D. Gautam and S. Katwal, "Book: Wavelet Transform- Spectrum Sensing", Technological Institute of High Studies Chalco, 2022.

22. B. I. S. Ronica, R. Sudharshanan, and etal, "Modified UWB for BER Reduction Using HAAR Wavelet Transform," *International Journal of, Applied Engineering Research*, Vol. 9, No.18, pp. 4515–4532, 2014.

23. M. Farhang and J. A. Salehi, "Optimum Receiver Design for Transmitted-Reference Signaling", *IEEE Trans. on Communication*, Vol. 59, pp. 1589-1598, 2011.

24. A. L. Emmanuel, "Thesis: Signal Processing for Transmitted-Reference Ultra-Wideband Systems", Toronto Metropolita*n University*, 2022.

25. Y. Chen and N. C. Beaulieu, "Improved Receivers for Generalized UWB Transmitted Reference Systems", *IEEE Trans. Wireless Commun.*, Vol. 7, pp. 500-504, 2008.

26. K. Muthukrishnan, M. Kamruzzaman, S. Lavadiya, V. S. Thoya, "Superlative split ring resonator shaped ultrawideband and high gain 1×2 MIMO antenna for Terahertz communication, Nano Communication Networks", 2023, 100437.

27. A. Pandey, A. P. Singh, V. Kumar, "Design and optimization of circularly polarized dielectric resonator-based MIMO antenna using machine learning for 5G Sub-6 GHz", *AEU - International Journal of Electronics and Communications*, Vol. 162, April 2023, 154558.

28. M. I. Ahmed, M. F. Ahmed, and H. Seleem, "Channel Capacity and Polarization Diversity Study for Novel Compact UWB MIMO Antennas", *International Journal of Microwave and Optical Technology*, Vol.16, No.4, 2021.

29. M. Wasim, S. Khera, P. K. Malik, S. V. Kumari, S. D., Walid El-Shafai and M. H. Aly, "Base Station MIMO Antenna in 1 × 6 Array Configurations with Reflector Design for Sub-6 GHz 5G Applications", *Electronics* , Vol. 12, No. 669. pp. 1-11, 2023.